

## Variability of Citrus Exocortis Viroid (CEVd)

M. Gandía, A. Palacio, and N. Duran-Vila

**ABSTRACT.** Single-strand conformation polymorphism (SSCP) has been adopted as a tool for viroid characterization. Nucleic acid extracts from a viroid field isolate containing CEVd was subjected to retrotranscription and PCR amplification using a set of contiguous CEVd-specific primers. The analysis of cloned DNAs recovered from this isolate illustrates the extent of variability within a single CEVd isolate. The relationship between the SSCP profiles observed among clones and the variation in their nucleotide sequences was confirmed by sequence analysis of selected clones. The results indicate that field isolates are complex populations or quasispecies. Two highly conserved sequences (master sequences) as well as several less abundant variants were consistently identified. The sequence variants presented a base pairing arrangement in the P domain characteristic of severe strains of CEVd. A branched secondary structure rather than the rod-like structure was predicted to occur at 37°C.

*Index words.* Variants, SSCP, quasispecies.

Citrus exocortis viroid (CEVd), the causal agent of the exocortis disease, was discovered in 1972 (12). Determination of its primary structure (4, 14), showed that the CEVd molecule is a covalently closed circular RNA with a highly base paired rod-like structure which conforms the model of five structural domains ( $T_L$ , P, C, V,  $T_R$ ) (7).

Viroid replication which occurs in the absence of proof-reading mechanisms accounts for a high rate of variability generation. Although there are numerous structural constraints, which impair infectivity and/or replication ability of specific viroid sequences, the information available indicates that CEVd may infect susceptible hosts as a number of different sequence variants (15).

Single-stranded conformation polymorphism analysis (SSCP) is based on the fact that partially denatured, double-stranded DNA (dsDNA) migrates as two single stranded DNA (ssDNA) bands in non-denaturing polyacrylamide gel electrophoresis (PAGE). The migration of the two ssDNA strands depends on their conformation under the PAGE conditions chosen. It has been demonstrated recently that SSCP analysis of full length viroid DNA can be used as a tool for a preliminary identification of sequence variants in studies that require extensive sequencing (11).

The objective of this study was to assess the variability of a well characterized field isolate of CEVd.

### MATERIALS AND METHODS

**Viroid source and extraction procedure.** The CEVd containing field isolate E-117 was inoculated on the selection 861-S1 Etrog citron grafted onto rough lemon rootstock. Inoculated citrons showing the characteristic symptoms of stunting, leaf epinasty and midvein necrosis were kept in a greenhouse at 28° to 32°C for at least 6 mo before being used as a source of tissue.

Samples (5 g) of young leaves and stems were homogenized in 5 ml volume of extraction buffer (0.4M Tris-HCl, pH 8.9; 1% (w/v) SDS; 5 mM EDTA, pH 7.0; 4% (v/v) mercaptoethanol) and 15 ml of water saturated phenol (13). The total nucleic acids were partitioned in 2M LiCl and the soluble fraction was concentrated by ethanol precipitation and resuspended in TKM buffer (10mM Tris-HCl; 10mM KCl; 0.1mM  $MgCl_2$ ; pH 7.4). Aliquots of nucleic acid preparations from citrons inoculated with CEVd and from non inoculated controls were analyzed by slot-blot hybridization to confirm CEVd infection and were used for cDNA synthesis.

**Infectivity assays.** Infectivity assays were performed on tomato, *Gynura aurantiaca*, and trifoliolate orange. Tomato and trifoliolate orange were propagated as seedlings and *G. aurantiaca* as rooted cuttings. Tomato and *G. aurantiaca* plants were slash inoculated with nucleic acid preparations from inoculated citrons and were kept in the greenhouse at 28° to 32°C. Trifoliolate orange seedlings were graft inoculated with citron tissues. Inoculated trifoliolate orange plants and uninoculated controls were transplanted to the field for symptom observation.

**cDNA synthesis and cloning.** CEVd cDNA was synthesized essentially as described by Yang et al. (16). First strand synthesis was performed using the CEVd-specific synthetic oligonucleotide (CEVd-1) complementary to bases 81 to 98 of CEVd-A (14) using Moloney Murine Leukemia Virus reverse transcriptase (M-MLV RT) (Promega Corp., Madison, WI). Second strand synthesis and amplification of dsDNA was performed with the synthetic oligonucleotides CEVd-1 and CEVd-2 in a buffer containing 1mM MgCl<sub>2</sub>, 0.25mM dNTPs, 0.5mM of each primer and 1 U of Taq DNA polymerase. PCR parameters consisted of 30 cycles of 92°C for 30 sec, 45°C for 1 min and 72°C for 2 min, with a final extension at 72°C for 15 min. The size of the DNA product was determined by electrophoresis in 2% agarose gels and its homology with CEVd was confirmed by slot-blot hybridization. The purified DNA was ligated to the thymidylated EcoRV site of the pT7-Blue vector (Novagen). Plasmids from transformed cells were subjected to restriction analysis to verify the presence of an insert of the expected size.

**SSCP analysis.** Cloned viroid dsDNA was recovered from the plasmids by PCR amplification using the same conditions described above. Two ml of the PCR products were mixed with 20 ml of the denaturing solution (90% formamide, 25

mM EDTA, 0.05% xylene-cyanole and 0.05% bromophenol blue), heated for 10 min at 100°C and chilled on ice. Denatured DNA was subjected to 14% PAGE (14 × 11.5 × 0.075 cm gels) in TBE buffer (89mM Tris-Borate, 2mM EDTA, pH 8.3) at 200V constant voltage for 16 hr. The DNA bands were visualized by silver staining (6).

**Molecular hybridization.** Full length monomeric RNA probes complementary (cRNA) and homologous (hRNA) to the CEVd sequence were synthesized by a transcription reaction with T7 and T3 RNA-polymerases respectively, using DIG-labeled UTP (Boehringer Mannheim) and the pCEVd plasmid (kindly provided by Prof. H. L. Sanger, Max-Planck-Institut, Munchen) as template.

Aliquots of nucleic acid preparations from inoculated citron and RT-PCR products were denatured in 20% formaldehyde and transferred to positively charged Nylon (Boehringer Mannheim) membranes using a Hybri-slot filtration manifold (BRL), fixed by UV cross-linking and hybridized against a DIG labeled cRNA probe.

Samples subjected to SSCP analysis were electroblotted to positively charged Nylon membranes (Boehringer Mannheim) at 200mA for 1 h, directly from the SSCP gels, using a modified TBE buffer (40mM Tris, 40 mM Boric acid, 1mM EDTA, pH 8.3). The membranes were UV cross-linked and hybridized with DIG labeled cRNA and hRNA probes.

Prehybridization and hybridization were performed in 50% formamide and 6× SSPE as described by Maniatis et al. (9). The membranes were prehybridized at 42°C for 2 to 4 h and hybridized overnight at 65°C. After hybridization, they were washed twice in 2× SSC, 0.1% SDS at room temperature for 15 min, followed by another wash in 0.1 × SSC, 0.1% SDS for 60 min at 68°C. The DIG-labeled hybrids were detected

with an anti-DIG-alkaline phosphatase conjugate (Fab fragments) and visualized with the chemiluminescence substrate CSPD (Boehringer Mannheim).

**Sequence analysis.** Inserts from cloned viroid DNA were sequenced with the ABI PRISM DNA sequencer 377 (Perkin-Elmer). Alignment of multiple sequences was performed using the program Clustal V (5). Secondary structure analysis were obtained with the program MFOLD (circular version) from the GCG package (17).

## RESULTS

**Symptom expression on exocortis sensitive hosts.** CEVd inoculated tomato and *G. aurantiaca* plants developed severe symptoms of stunting and epinasty 4 wk after inoculation. Trifoliolate orange seedlings developed the characteristic bark scaling symptoms 5 yr after inoculation.

**Identification of CEVd variants by SSCP analysis.** When nucleic acid preparations from CEVd-infected citrons were subjected to retrotranscription and PCR amplification using CEVd-1 and CEVd-2 primers, a monomeric CEVd-DNA product was recovered.

The CEVd-DNA was ligated to the pT7-Blue vector and 316 clones containing full-length inserts were obtained.

SSCP analysis of the 316 clones revealed the existence of different electrophoretic profiles representatives of which are shown in Fig. 1A. Molecular hybridization of electroblotted samples using cRNA and hRNA probes (Fig. 1B and 1C) identified the rapidly migrating band as dsDNA and at least two stable conformations of the cDNA and hDNA strands. The slowly migrating cDNA and hDNA strands were very similar in electrophoretic mobility and were usually observed as a doublet in the upper part of the gel. The more rapidly migrating cDNA and hDNA species were chosen for discrimination of CEVd variants (see arrows in Fig. 1A). Based on this SSCP analysis approach, 44 variants were identified.

**Primary and secondary structures.** These 44 variants were further characterized by sequence analysis of selected clones. A master sequence (variant 1), with 98.65% and 98.12% homologies with CEVd-C (4) and CEVd-A (14), respectively, represented 52.8% (167 clones) of the population. From the remaining clones, 38.9% (123 clones)

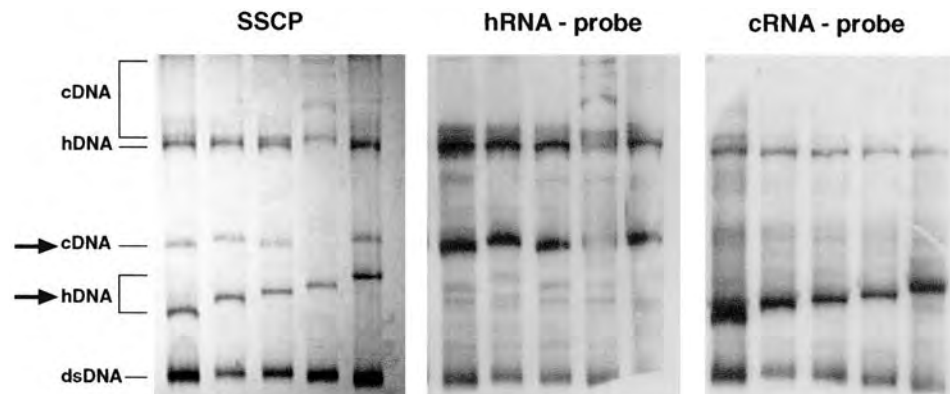


**Fig. 1.** SSCP analysis and molecular hybridization of cloned viroid sequences showing different SSCP profiles: (A) SSCP gel; (B) Hybridization of electroblotted samples against a DIG-labeled hRNA probe; (C) Hybridization of electroblotted samples against a DIG-labeled cRNA probe.

contained a single change at position 75. Deviations from the master sequence affected all the viroid structural domains. Most of the changes affected the pathogenicity (P) and variable (V) domains (found in 29 and 13 of the variants, respectively). Changes in the central (C) and terminal domains ( $T_R$  and  $T_L$ ) were infrequent. No additional variation was found when several clones presenting the dominant SSCP profiles (variants 1 and 2) which represent together 78% of the population, were sequenced. Alignment of these 44 sequence variants with CEVd-J and CEVd-30, representatives of class A and class B respectively, defined by Visvader and Symons (15), revealed that all were highly homologous to class A.

The distribution of the sequence changes which were found in at least two separate clones is shown in Fig. 2. From the nucleotide changes discriminating class A and class B (15), these variants presented 18 changes

as in class A (shown in italics in Fig. 3) and 5 changes as in class B (shown in bold in Fig. 3). In addition these sequences presented 7 nucleotide changes distinct from both class A and class B (shaded in Fig. 3).

These sequence variants were subjected to the MFOLD analysis, and as expected, the structure of minimum free energy at 25°C and 30°C was a highly base paired rod-like structure (Fig. 4A). However, the minimum free energy structure at 37°C was a branched structure resulting from rearrangements within  $T_L$  domain (Table 1; Fig. 4B).

The P domain of all the variants analyzed presented primary and secondary structures similar to the CEVd variants classified as class A by Visvader and Symons (15) (Fig. 5). The changes identified in the P domain always affected the pathogenicity modulating region (PL) (15). Deviations from the structure of the master sequence (variant 1) can be summarized as follows: a) Variants 5

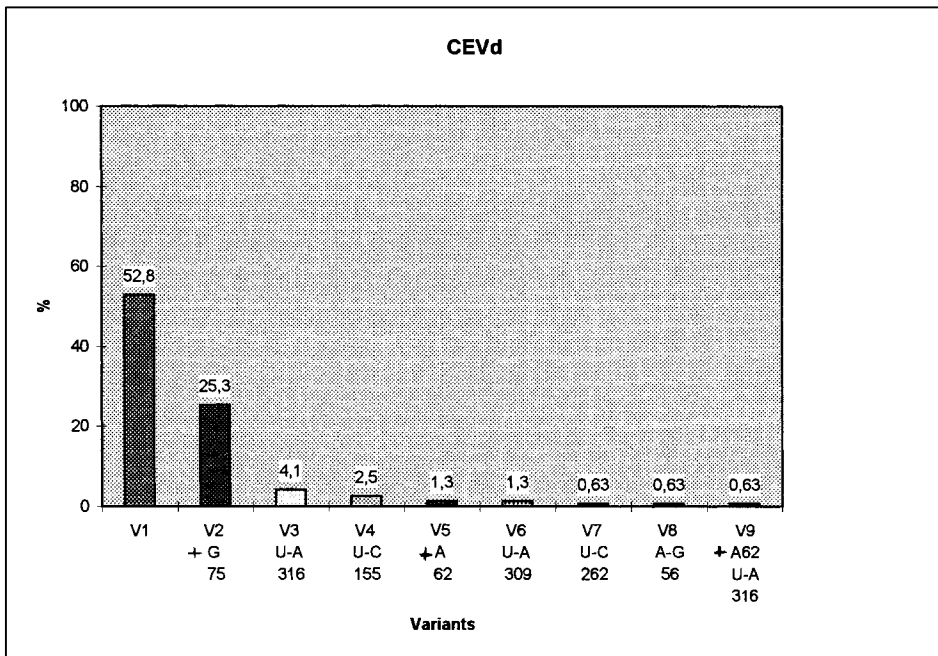
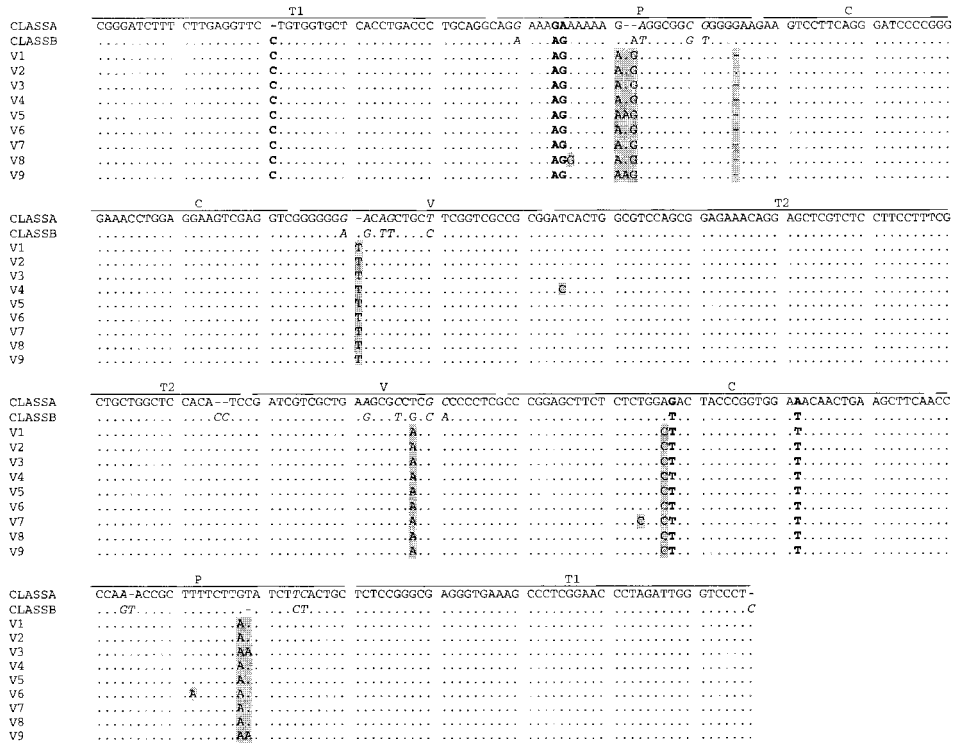


Fig. 2. Frequency of sequence variants represented by two or more clones, and changes (exchange or insertion) respect to the dominant variant 1 (master sequence).



**Fig. 3. Aligning of different variants (V1 to V9) with sequences of class A and B defined by Visvader and Symons (15). Nucleotides characteristic of class A (italics) and class B (bold). Nucleotide changes distinct from class A and class B (shaded).**

and 9 which contain an addition +A in nucleotide 62 and a change U→A at position 316 in variant 9 contain an enlarged poly-A loop; b) Variant 2

which contain an addition +G at position 75 contain an enlarged right loop; c) Variants 3, 6 and 8 which contain single change U→A at posi-

**TABLE 1**  
MINIMUM FREE ENERGY AND SECONDARY STRUCTURES OF DIFFERENT CEVD SEQUENCE VARIANTS

Variant	25°C		30°C		37°C	
	Structure	Energy (Kcal mol <sup>-1</sup> )	Structure	Energy (Kcal mol <sup>-1</sup> )	Structure	Energy (Kcal mol <sup>-1</sup> )
Class A <sup>a</sup>	Rod	-171.6	Rod	-149.3	Rod	-122.6
Class B <sup>a</sup>	Rod	-173.3	Rod	-151.3	Rod	-124.6
Variant 1	Rod	-173.8	Rod	-151.4	Branched	-125.1
Variant 2	Rod	-173.8	Rod	-151.4	Branched	-125.1
Variant 3	Rod	-173.8	Rod	-151.4	Branched	-125.1
Variant 4	Rod	-172.1	Rod	-149.8	Branched	-123.7
Variant 5	Rod	-173.4	Rod	-151.0	Branched	-124.6
Variant 6	Rod	-173.8	Rod	-151.4	Branched	-125.1
Variant 7	Rod	-175.9	Rod	-153.5	Branched	-127.4
Variant 8	Rod	-173.5	Rod	-151.1	Branched	-125.0
Variant 9	Rod	-174.4	Rod	-151.0	Branched	-124.7

<sup>a</sup>Visvader and Symons (15).

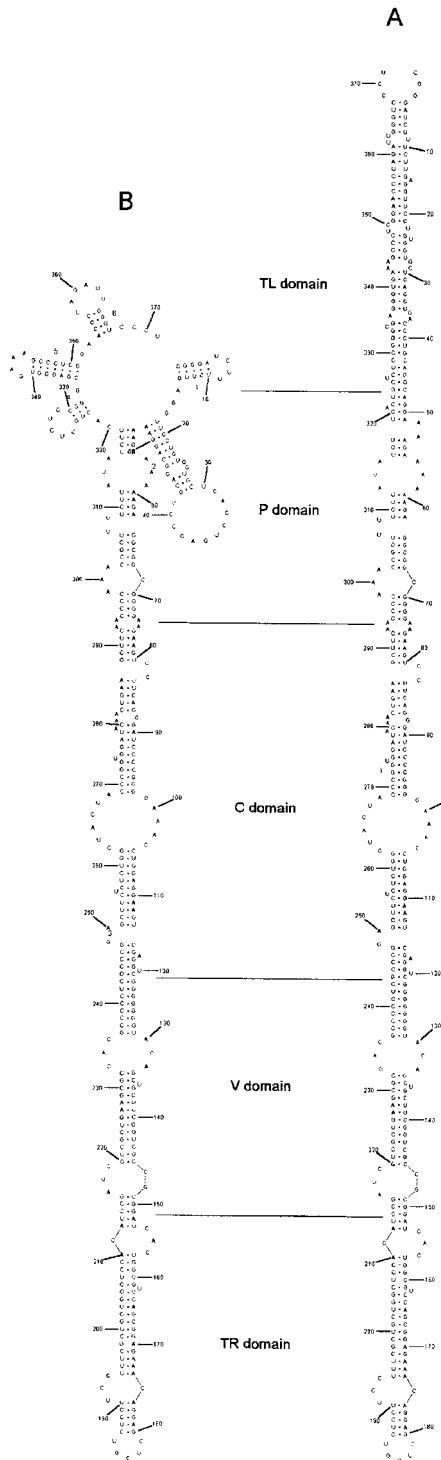


**Fig. 4.** Secondary structures of the dominant CEVd sequence (variant 1), as predicted by the MFOLD program, at 25°C (A) and 37°C (B).

	AA	AAA		CG	A	
46	GCAG	GA	AGA	AAGA	GGCGG	GGGG 75
325	CGUC	CU	UCU	UUCU	UCGCC	CCCC 294
	A		AUG	UU	AAA	A
<b>A</b>						
	AAAA	AA	U	GG	A	
46	GCAG	GA	AGA	AAGA	GGCGG	GGGG 75
325	CGUC	CU	UCU	UUCU	UCGCC	ACCCC 295
		AUC	AG	UU	AUG	A
<b>B</b>						
	AA	AAA		C	A	
46	GCAG	GA	AGA	AAGA	GGCGG	GGGG 74
325	CGUC	CU	UCU	UUCU	UCGCC	CCCC 294
	A		AUA	UU	AAA	A
<b>V1</b>						
	AA	AAA		CG	A	
46	GCAG	GA	AGA	AAGA	GGCGG	GGGG 75
325	CGUC	CU	UCU	UUCU	UCGCC	CCCC 294
	A		AUA	UU	AAA	A
<b>V2</b>						
	AA	AAA		C	A	
46	GCAG	GA	AGA	AAGA	GGCGG	GGGG 74
325	CGUC	CU	UCU	UUCU	UCGCC	CCCC 294
	A		AAA	UU	AAA	A
<b>V3</b>						
	AA	AAAA		C	A	
46	GCAG	GA	AGA	AAGA	GGCGG	GGGG 75
326	CGUC	CU	UCU	UUCU	UCGCC	CCCC 295
	A		AUA	UU	AAA	A
<b>V5</b>						
	AA	AAA		C	A	
46	GCAG	GA	AGA	AAGA	GGCGG	GGGG 74
325	CGUC	CU	UCU	UUCU	UCGCC	CCCC 294
	A		AUA	UA	AAA	A
<b>V6</b>						
	AA	AAA		C	A	
46	GCAG	GA	GGA	AAGA	GGCGG	GGGG 74
325	CGUC	CU	UCU	UUCU	UCGCC	CCCC 294
	A		AUA	UU	AAA	A
<b>V8</b>						
	AA	AAAA		C	A	
46	GCAG	GA	AGA	AAGA	GGCGG	GGGG 75
326	CGUC	CU	UCU	UUCU	UCGCC	CCCC 295
	A		AAA	UU	AAA	A
<b>V9</b>						

**Fig. 5.** Secondary structure of the P domain of different sequence variants (V1 to V9) containing changes in this domain, as compared to the class A and B defined by Visvader and Symons (14).

tion 316, U→A change at position 309 and A→G change at position 56 respectively, did not result in modifications of the secondary structure.

**DISCUSSION**

Like PSTVd (3), CEVd confirms the “quasispecies model” proposed by Eigen (2) to describe heterogeneous populations of RNA molecules. The CEVd population we examined contains a best single

variant (master sequence) representing 52.8% of the population and 43 sequence variants, most of which are represented by single clones. Secondary structures indicated that the P domain of variants studied, exhibited the same base pairing pattern as the class A variants defined by Visvader and Symons (15) which included CEVd sequences that induced severe symptoms in tomato.

Sequence variants of PSTVd with structural differences in the "PM loop" (so-called Pathogenicity Modulating) were also identified as naturally occurring (8) or recovered by site directed mutagenesis (10) and were demonstrated to be responsible on differences in symptom induction and sequence stability. Although the CEVd variants identified in this study conform to the structure of the severe class A, the changes identified in the P domain may also affect the pathogenesis and sequence stability of specific variants. With the availability of the cloned sequences further studies on the pathogenicity of CEVd can be pursued. Most of the studies to date have focused on symptom expression on tomato as an experimental host, which displays symptoms distinct from the bark scaling syndrome of the exocortis disease. Therefore, further efforts must be devoted to the

understanding of the pathogenicity determinants of the CEVd molecule in citrus hosts.

Bussière et al., (1) described a branched secondary structure in CEVd, which was located at the left extremity. MFOLD analysis revealed that unlike the CEVd sequences of class A and class B, all the variants appear to be able to fold into a branched secondary structure. Therefore, the specific nucleotide changes characteristic of this variants must be implicated in the adoption of the branched conformation. This observation suggests that structures other than the rod-like structure may also operate *in vivo*, thus providing additional binding sites to interact with putative receptors of the host plant.

As a result of this work, cDNA clones containing sequence changes affecting specific domains of the viroid molecule are available to pursue their further biological characterization by infectivity studies.

## ACKNOWLEDGMENT

The authors acknowledge the technical assistance of Victor Real and Niceto Muñoz on the analysis of secondary structures. This work was supported by INIA grant 1712 and a IVIA fellowship to the first author.

## LITERATURE CITED

1. Bussière, F., D. Lafontaine, and J. P. Perrault  
1996. Compilation and analysis of viroid and viroid-like RNA sequences. *Nucleic Acids Res.* 24: 1793-1798.
2. Eigen, M.  
1993. The origin of genetic information: Viruses as models. *Gene* 135: 37-47.
3. Góra-Sochacka, A., A. Kierzez, T. Candresse, and W. Zagórski  
1997. The genetic stability of potato spindle tuber viroid (PSTVd) molecular variants. *RNA* 3: 68-74.
4. Gross, H. J., G. Krupp, H. Domdey, M. Raba, P. Jank, C. Lossow, H. Alberty, K. Ramm, and H. L. Sänger  
1982. Nucleotide sequence and secondary structure of citrus exocortis and chrysanthemum stunt viroid. *Eur. J. Biochem.* 121: 249-257.
5. Higgins, P. G. and P. M. Sharp  
1989. Fast and sensitive multiple sequence alignment on a microcomputer. *Comp. Appl. Biosci.* (CABIOS) 5: 151-153.
6. Igloi, G. L.  
1983. Silver stain for the detection of nanogram amounts of tRNA following two-dimensional electrophoresis. *Anal. Biochem.* 134: 184-188.

7. Keese, P. and R. H. Symons  
1985. Domains in viroids: Evidence of intermolecular RNA rearrangements and their contribution to viroid evolution. *Proc. Natl. Acad. Sci. USA* 82: 4582-4586.
8. Lakshman, D. K. and S. M. Tavantzis  
1993. Primary and secondary structure of a 360-nucleotide isolate of potato spindle tuber viroid. *Arch. Virol.* 128: 319-331.
9. Maniatis, T., E. F. Fritsch, and J. Sambrook  
1989. *Molecular Cloning: A Laboratory Manual, 2d Ed.* Cold Spring Harbor Laboratory, N.Y.
10. Owens, R. O., W. Chen, Y. Hu, and Y. H. Hsu  
1995. Suppression of potato spindle tuber viroid replication and symptom expression by mutations which stabilize the pathogenicity domain. *Virology* 208: 554-564.
11. Palacio, A. and N. Duran-Vila  
1999. Single-strand conformation polymorphism (SSCP) analysis as a tool for viroid characterisation. *J. Virol. Methods* 77: 27-36.
12. Semancik, J. S. and L. G. Weathers  
1972. Exocortis virus: an infectious free nucleic acid plant virus with unusual properties. *Virology* 47: 456-466.
13. Semancik, J. S., T. J. Morris, L. G. Weathers, G. F. Rordorf, and D. R. Kearns  
1975. Physical properties of a minimal infectious RNA (viroid) associated with the exocortis disease. *Virology* 63: 160-167.
14. Visvader, J. E., A. R. Gould, G. E. Bruening, and R. H. Symons  
1982. Citrus exocortis viroid: Nucleotide sequence and secondary structure of an Australian isolate. *FEBS Lett.* 137: 288-292.
15. Visvader, J. E. and R. H. Symons  
1985. Eleven new sequence variants of citrus exocortis viroid and the correlation of sequence with pathogenicity. *Nucleic Acids Res.* 13: 2907-2920.
16. Yang, X., A. Hadidi, and S. M. Garnsey  
1992. Enzymatic cDNA amplification of citrus exocortis and cachexia viroids from infected citrus hosts. *Phytopathology* 82: 279-285.
17. Zuker, M.  
1989. On finding all suboptimal foldings of an RNA molecule. *Science* 244: 48-52.